EAST EUROPEAN JOURNAL OF PHYSICS. 4. 590-600 (2025)
DOI:10.26565/2312-4334-2025-4-62 ISSN 2312-4334

INPUT CHARACTERISTICS OF ELECTRICALLY THIN DIPOLE WITH VARIABLE RADIUS ALONG ANTENNA LENGTH

Mikhail V. Nesterenko*, Oleksandr M. Dumin, Yurii V. Arkusha
V.N. Karazin Kharkiv National University, 4, Svobody Sq., Kharkiv, Ukraine, 61022
**Corresponding Author: mikhail.v.nesterenko@gmail.com*
Received July 1, 2025; revised November 5, 2025; accepted November 15, 2025

An approximate analytical solution to the problem of radiation (diffraction) of electromagnetic waves by dipole (monopole) with variable radius along antenna length is presented. The solution was carried out using generalized method of induced electromotive forces (EMF). An influence of the change of monopole radius upon input characteristics is numerically studied. Theoretical results are compared with the experimental data.
Keywords: *Dipole; Monopole; Variable radius; Input characteristics; Generalized method of induced EMF*
PACS: 02.70.Pt; 78.70Gq; 84.40.-x

An additional parameter for obtaining the given electrodynamic characteristics of cylindrical dipole (monopole) antennas can be the change of the radius of the cross-section of the dipole along its length. Such radiators can be located in free space (dipole), half-space (monopole), rectangular waveguide, resonator, on sphere etc. Suppose the radius of the dipole increases from the center of the antenna to its ends according to a linear law (biconical dipole, conical monopole). In that case, such an antenna resonates at a shorter geometric length and is more broadband than a dipole of constant radius. Starting from the classic publications of Schelkunoff [1], Tai [2], Woodward & Brown [3], Bevensee [4], antennas of this type have attracted the attention of many researchers. These can be symmetrical radiators excited by a point source [5], [6], [7], [8], [9], [10]; dipoles with asymmetrical arms [11], [12], antennas with asymmetrical arms and excitation [13], [14], [15], [16]; modified radiators with minor design changes compared to traditional designs [17], [18], [19], [20]; as well as passive scattering antenna elements [21], [22], [23], [24], [25]. However, all of them are devoted to calculating the characteristics of a radiating (scattering) dipole (monopole) with a linear law of the change of antenna radius.

In this paper, an approximate analytical solution to the problem of radiation (scattering) of electromagnetic waves by a dipole (monopole) with other laws of change of radius along antenna length (piecewise linear (diamond-shaped), Vivaldi type, combined trigonometric, circle, piecewise constant) is presented. The solution was carried out using the generalized method of induced electromotive forces (EMF) in accordance with the concept of "thin-wire approximation". The input characteristics of the antennas under consideration are analyzed in detail.

PROBLEM FORMULATION AND INTEGRAL EQUATION SOLUTION

Let the monopole of the L length and the variable radius $r(s)$, located in half-space, be excited by the electric field extraneous source $E_{0s}(s)$ (Fig. 1). The monochromatic fields and currents depend on time t as $e^{i\omega t}$ ($\omega = 2\pi f$ is the circular frequency, f is the frequency, measured in Hz). The monopole is electrically thin, if the following inequalities are performed:

$$kr(s) << 1,\ r(s) << 2L, \tag{1}$$

where $k = 2\pi/\lambda$, λ is the wavelength in free space.

The integral equation in the current $J(s)$ for the impedance boundary condition on the dipole surface acquires the form [6], [24]:

$$\left(\frac{\mathrm{d}^2}{\mathrm{d}s^2} + k^2\right)\int_{-L}^{L} J(s')\frac{e^{-ik\tilde{R}(s,s')}}{\tilde{R}(s,s')}\mathrm{d}s' = -\frac{i\omega}{\cos\psi}\left[E_{0s}(s) - z_i J(s)\right]. \tag{2}$$

Here $\tilde{R}(s,s') = \sqrt{(s-s')^2 + r^2(s)}$, s and s' are the local coordinates related to the dipole axis and surface, z_i is the distributed internal linear impedance, $J(\pm L) = 0$, $-L$ is the coordinate of the mirror image of the dipole relative to the infinite ideally conducting plane (for monopole). So, for example, for metal cylinders (σ is the metal conductivity, Δ^{o} is the skin layer thickness) under the condition $r >> \Delta^{\mathrm{o}}$, is determined by the relation $z_i = \dfrac{1+i}{2\pi r\sigma\Delta^{\mathrm{o}}}$. Despite the fact that

Cite as: M.V. Nesterenko, O.M. Dumin, Y.V. Arkusha, East Eur. J. Phys. 4, 590 (2025), https://doi.org/10.26565/2312-4334-2025-4-62

for real metals the values z_i are quite small, it is necessary to take this term into account. In this case, equation (2) is the Fredholm equation of the 2-nd kind and has a unique solution. Note also that at $r(s) = const = r_0$, equation (2) transforms into the equation in the current along an impedance dipole of constant radius with a quasi-one-dimensional core $\tilde{R}(s,s') = R(s,s') = \sqrt{(s-s')^2 + r_0^2}$.

The approximate analytical solution of the equation (2) can be obtained by the generalized method of induced EMF [13], [14]. Note that in [24] equation (2) for a symmetric biconical dipole is solved by means of the averaging method [26]. Using this method the approximating current distribution functions in expressions (3) were also found.

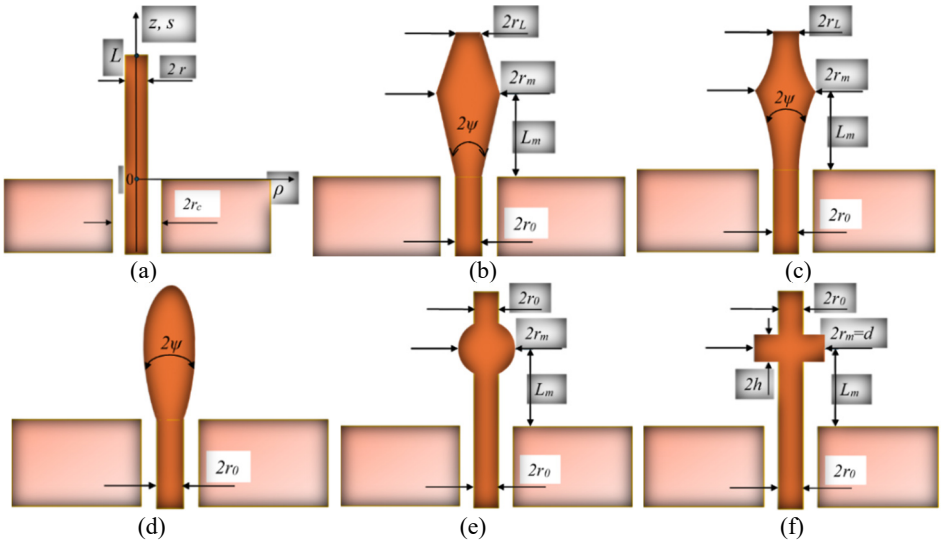

Figure 1. The problem geometry and corresponding notations: (a) - constant radius; (b) - (f) - variable radius

The dipole currents can be presented as product of the unknown complex amplitudes J_n and distribution functions $f_n(s)$ ($n = 0,1$) as

$$J(s) = J_0 f_0(s) + J_1 f_1(s); \quad f_n(\pm L) = 0. \tag{3}$$

Then the approximate solution to equation (2) can be obtained in the form ($m,n = 0,1$)

$$J(s) = -\frac{i\omega}{2k\cos\psi}\left[J_0 f_0(s) + J_1 f_1(s)\right], \tag{4}$$

where $J_0 = \dfrac{E_0 Z_{11}^{\Sigma} - E_1 Z_{01}^{\Sigma}}{Z_{00}^{\Sigma} Z_{11}^{\Sigma} - Z_{10}^{\Sigma} Z_{01}^{\Sigma}}$, $J_1 = \dfrac{E_1 Z_{00}^{\Sigma} - E_0 Z_{10}^{\Sigma}}{Z_{00}^{\Sigma} Z_{11}^{\Sigma} - Z_{10}^{\Sigma} Z_{01}^{\Sigma}}$,

$$Z_{mn} = \frac{1}{2k\cos\psi}\left\{-\frac{\mathrm{d}f_m(s)}{\mathrm{d}s}A_n(s)\Big|_{-L}^{L} + \int_{-L}^{L}\left[\frac{\mathrm{d}^2 f_m(s)}{\mathrm{d}s^2} + k^2 f_m(s)\right]A_n(s)\mathrm{d}s\right\}, \quad A_n(s) = \int_{-L}^{L} f_n(s')\frac{e^{-ik\tilde{R}(s,s')}}{\tilde{R}(s,s')}\mathrm{d}s', \tag{5a}$$

$$\tilde{Z}_{mn} = -\frac{i\omega}{2k\cos\psi}\int_{-L}^{L} f_m(s) f_n(s) z_i \,\mathrm{d}s, \quad Z_{mn}^{\Sigma} = Z_{mn} + \tilde{Z}_{mn}, \quad E_m = \int_{-L}^{L} f_m(s) E_{0s}(s)\mathrm{d}s. \tag{5b}$$

Let the dipole be excited in the point $s = 0$ by the voltage generator with amplitude V_0: $E_{0s}(s) = V_0\delta(s-0)$, where δ is the Dirac delta function. Let us choose the functions $f_{0,1}(s)$ according to [26] in the following form:

$$f_0(s) = \sin\tilde{k}(L - |s|), \quad f_1(s) = \cos\tilde{k}s - \cos\tilde{k}L, \tag{6}$$

where $\tilde{k} = k - \dfrac{iz_i[3/2 - r_0/(2r_m)]}{120\cos\psi\ln(2L/r_m)}$, r_0 and r_m are the radii of the dipole in points $s = 0$ and $s = L_m$ (Fig. 1). Note that the approximation of functions (6) adequately represents the real physical process if the dipole electrical lengths are small

$(2L/\lambda) \le 1.4$ [26]. Other approximating function [26] $f_2^s(s) = \cos(ks/2) - \cos(kL/2)$ is valid in the range $1.4 < (2L/\lambda) \le 2.5$.

The coefficients Z_{mn}^{Σ} in the formulas (4) can be obtained from expressions (5), (6):

$$Z_{0n} = \frac{\tilde{k}[A_n(L) - \cos\tilde{k}LA_n(0)]}{k\cos\psi} + \frac{k^2 - \tilde{k}^2}{2\cos\psi}\int_{-L}^{L} f_0(s)A_n(s)\mathrm{d}s,\ Z_{1n} = \frac{\tilde{k}\sin\tilde{k}LA_n(L)}{k\cos\psi} - \frac{1}{2k\cos\psi}\begin{bmatrix} k^2\cos\tilde{k}L\int_{-L}^{L} A_n(s)\mathrm{d}s \\ -(k^2-\tilde{k}^2)\int_{-L}^{L}\cos\tilde{k}sA_n(s)\mathrm{d}s \end{bmatrix}$$

$$\tilde{Z}_{00} = -\frac{i\omega\varepsilon_i(2\tilde{k}L - \sin 2\tilde{k}L)}{2k\tilde{k}\cos\psi},\ \tilde{Z}_{01} = \tilde{Z}_{10} = -\frac{i\omega\varepsilon_i[\tilde{k}L\sin\tilde{k}L - 2\cos\tilde{k}L(1-\cos\tilde{k}L)]}{k\tilde{k}\cos\psi},$$

$$\tilde{Z}_{11} = -\frac{i\omega\varepsilon_i[2\tilde{k}L - 3\sin 2\tilde{k}L + 4\tilde{k}L\cos^2\tilde{k}L]}{2k\tilde{k}\cos\psi},\ E_0 = \sin\tilde{k}L,\ E_1 = 1 - \cos\tilde{k}L.$$

The input impedance for monopole $Z_{in} = R_{in} + iX_{in}$ and admittance $Y_{in} = G_{in} + iB_{in}$ can be presented as

$$Z_{in}[\mathrm{Ohm}] = \frac{30i}{J_0 f_0(0) + J_1 f_1(0)},\qquad Y_{in}[\mathrm{mS}] = \frac{10^3}{Z_{in}} \tag{7}$$

Then, the module of reflection coefficient in the antenna feeder with the wave impedance W is equal to

$$|S_{11}| = \left|\frac{Z_{in} - \mathrm{W}}{Z_{in} + \mathrm{W}}\right|, \tag{8}$$

and the voltage standing wave ratio is determined by the formula $\mathrm{VSWR} = (1 + |S_{11}|)/(1 - |S_{11}|)$.

Note that for printed antennas of the type under consideration (piecewise linear (diamond-shaped), Vivaldi type, combined trigonometric, circle, piecewise constant), the solution to equation (2) is also valid, but it is necessary to make the replacement $r(s) = d(s)/4$ [26], where $d(s)$ is the antenna width.

NUMERICAL AND MEASURED RESULTS

Next we will consider radiators with the following geometric parameters [27]: r_0 =1.522 mm, r_c =3.5 mm, L =50.065 mm, $k\rho \to \infty$. Then the characteristic impedance of the feeder line is $\mathrm{W} = 60\ln(r_c/r_0)$ =50 Ohm. Fig. 2 shows the dependences of the real and imaginary parts of the input impedance of the regular and conical monopoles ($L_m = L$) on its electrical length at different angles ψ.

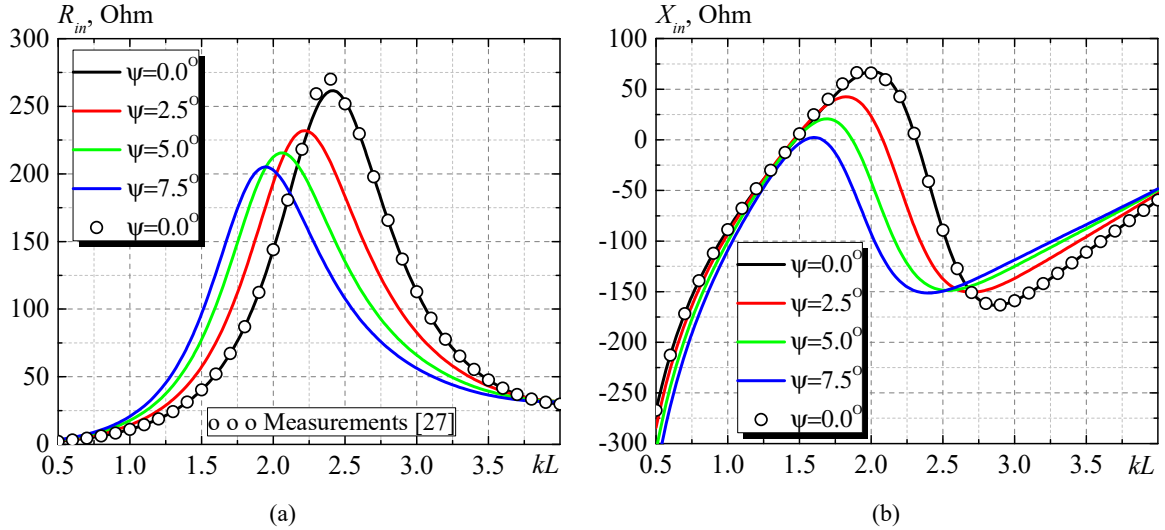

Figure 2. The dependences of the calculated (7) and measured [27] monopole input impedance on its electrical length at different angles ψ: (a) – real part R_{in}, (b) – imaginary part X_{in}

As can be seen, the agreement between the calculated and measured values $Z_{in}(kL)$ at $\psi = 0.0^{O}$ (regular monopole) is quite satisfactory, and with the increase of the angle ψ the impedance change trends to coincide with those measured in [3]. To satisfy inequalities (1), we will limit ourselves to the value $\psi = 7.5^{O}$ ($r_m = 8.038$ mm, $r_m / 2L = 0.08$).

1. Numerical results for piecewise linear law of $r(s)$

Fig. 3a shows the laws of change of radius along the monopole (Fig. 1b) determined by the following formula

$$r(s) = \begin{cases} r_0 + s\tan\psi, \text{ at } s \le \kappa L, \\ r_0 + [\kappa/(1-\kappa)](L-s)\tan\psi, \text{at } s \ge \kappa L, \end{cases} \tag{9}$$

where $\kappa = s_m / L$, and Fig. 3b shows the dependences of the reflection coefficient modulus $|S_{11}|$ in the feeder line corresponding to these laws. Fig. 3a also shows that curve $\kappa = 0.75$ has the longest path length on the surface of those presented there. Accordingly, this curve describes the resonance at the lowest frequency in Fig. 3b. However, the effect of this phenomenon on the resonance frequency is not always proportional to the increase in the path length. As for the minimum value of reflection observed for curve $\kappa = 0.25$, this can be explained by a relatively smooth bend at point L_m. It is also interesting that the shift of the resonant frequency in this case is proportional to the increase in the wave path along the dipole surface.

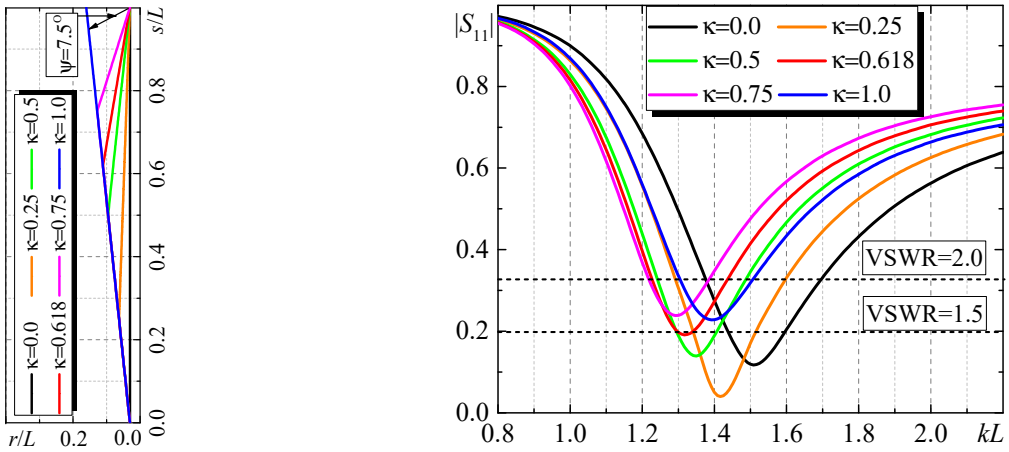

(a) (b)

Figure 3. The laws of change of radius along the monopole (a), the dependences of the reflection coefficient modulus $|S_{11}|$ in the feeder line from the electrical length of the monopole (b) at different positions of the maximum values of the radius and $\psi = 7.5^{O}$

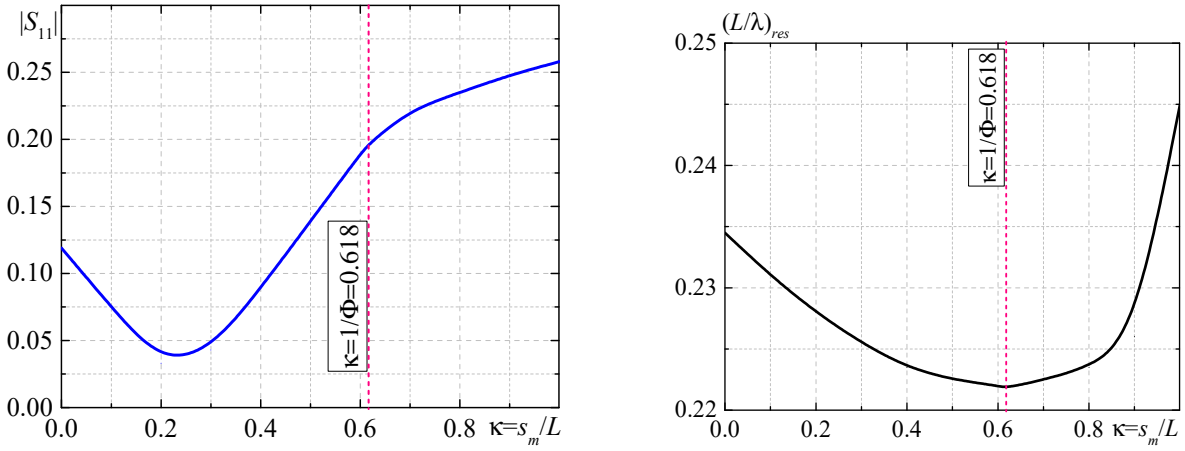

(a) (b)

Figure 4. The dependences of the reflection coefficient modulus $|S_{11}|$ on the coordinate of the point with the maximum radius along the length of the monopole (a), the dependences of the values of resonant "shortening" $(L/\lambda)_{res}$ on the coordinate of the point with the maximum radius along the length of the monopole at $\psi = 7.5^{O}$

Figs. 4 show the dependences of the reflection coefficient modulus $|S_{11}|$ and values of resonant "shortening" (the resonance condition is the fulfillment of equality $X_{in}=0$ when the sign X_{in} changes from negative to positive) $(L/\lambda)_{res}$ (compared to a tuned monopole, where $(L/\lambda)_{res}=0.25$) on the coordinate of the point with the maximum radius along the length of the monopole. In Figs. 4 the dotted line indicates the value $\kappa=0.618$ that is associated with the quantity $\kappa=1/\Phi$, where $\Phi=1.618$ is the so-called "golden ratio" [28]. As you can see, the value $\kappa\approx 0.618$ is a "inflection point" on both graphs. This can be explained by the fact that at this point the additional capacitance formed by the last segment of the monopole operates in an optimal way, which creates this shortening. Approximation of the function in Fig. 4a and the study of its derivatives indeed allow us to conclude that at $\kappa\approx 0.618$ there is an inflection point.

Placing the maximum values of the monopole radius at this point for different angles ψ (Fig. 5a) leads to an even better matching of the monopole with the feeder line (Fig. 5b).

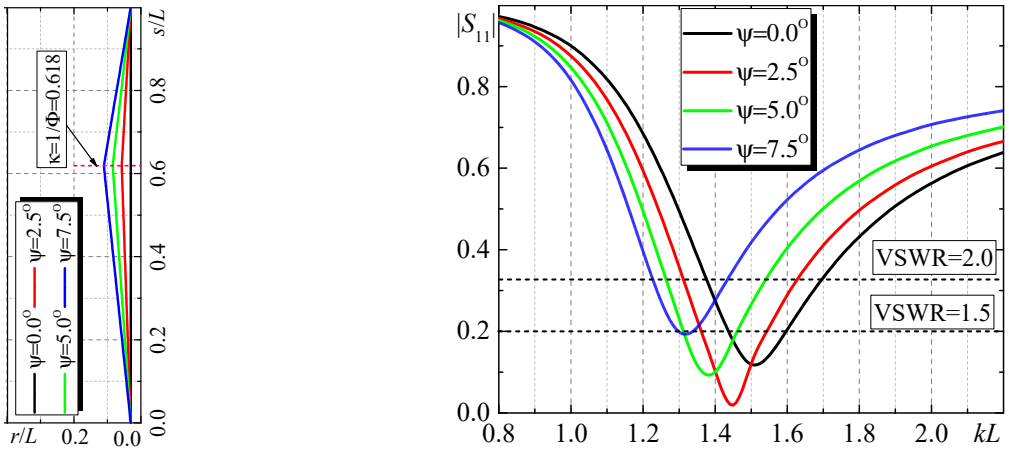

(a) (b)

Figure 5. The laws of change of radius along the monopole at $\kappa=0.618$ (a), the dependences of the reflection coefficient modulus $|S_{11}|$ in the feeder line from the electrical length of the monopole (b) for different ψ

2. Numerical results for Vivaldi type law of $r(s)$

Fig. 6a shows the laws of change in radius along the monopole, determined by the following formula (Vivaldi type antenna [29], Fig. 1c).

$$r(s)=\begin{cases} r_0+(1/\kappa)s\tan\psi e^{\beta(s/L-\kappa)}, \text{ at } s\le \kappa L, \\ r_0+[1/(1-\kappa)](L-s)\tan\psi e^{-\beta(s/L-\kappa)}, \text{at } s\ge \kappa L, \end{cases} \tag{10}$$

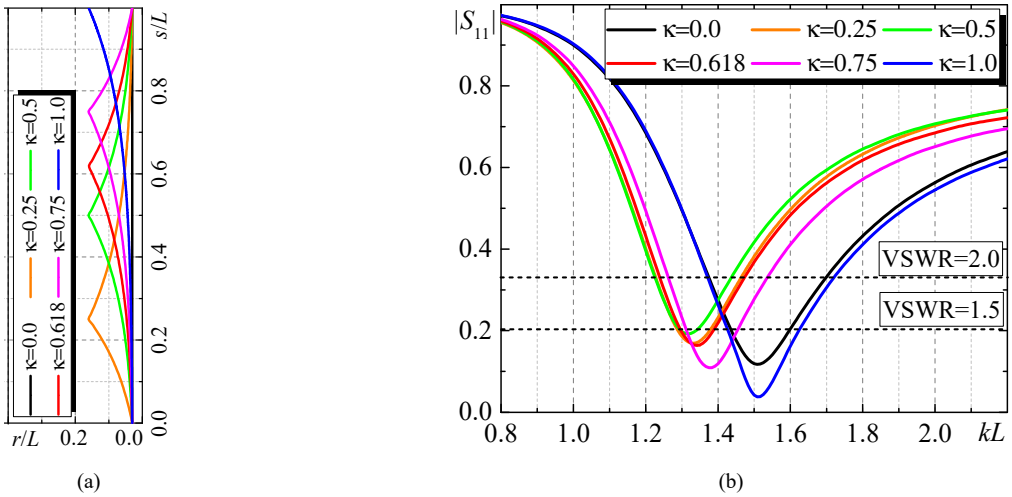

(a) (b)

Figure 6. The laws of change of radius along the monopole at $\psi=7.5^{\circ}$ and $\beta=\pi$ (a), the dependences of the reflection coefficient modulus $|S_{11}|$ in the feeder line from the electrical length of the monopole (b) for different κ

Fig. 6b shows the dependences of the reflection coefficient modulus $|S_{11}|$ in the feeder line corresponding to these laws. As can be seen, the best matching is observed at $\kappa = 1.0$ (conical monopole) with a practically unchanged resonant frequency compared to regular monopole ($\kappa = 0.0$, $r(s) = const$). In other cases, there is the decrease of the resonant frequency in comparison with a regular monopole. In Figs. 6 the red line indicates the value $\kappa = 0.618$. Fig. 7a shows the laws of change of radius along the monopole, determined by the formula (10) and $\kappa = 0.618$ for various β. Fig. 7b shows the dependences of the reflection coefficient modulus $|S_{11}|$ in the feeder line corresponding to these laws. As can be seen, the best matching is observed at $\beta = 4\pi$ and for all laws of change of radius the decrease is observed in the resonant frequency in comparison with a regular monopole.

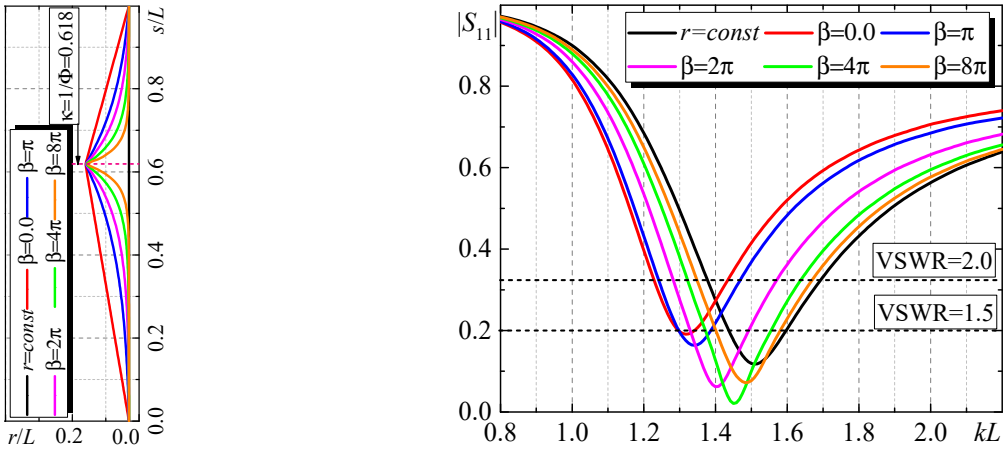

(a) (b)

Figure 7. The laws of change of radius along the monopole at $\psi = 7.5^{\circ}$ and $\kappa = 0.618$ (a), the dependences of the reflection coefficient modulus $|S_{11}|$ in the feeder line from the electrical length of the monopole (b) for different β

3. Numerical results for combined trigonometric law of $r(s)$

Let us further consider another law of change of radius along the monopole length, which is a combination of trigonometric functions [30] (Fig. 1d):

$$r(s) = r_0 + 4\kappa L \tan\psi \cos(\pi s / 2L)[1 - \cos(\pi s / 2L)]. \tag{11}$$

As can be seen, the best matching is observed at $\psi = 2.5^{\circ}$ (similar to Fig. 5b) and for all laws of change of radius a decrease is observed in the resonant frequency in comparison with a regular monopole.

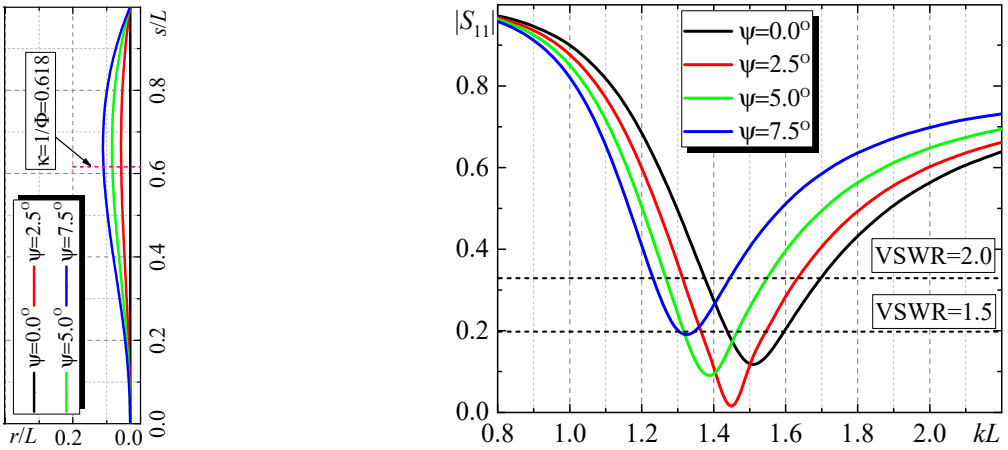

(a) (b)

Figure 8. The laws of change of radius along the monopole at $\kappa = 0.618$ (a), the dependences of the reflection coefficient modulus $|S_{11}|$ in the feeder line from the electrical length of the monopole (b) for different ψ

4. Numerical results for circle law of $r(s)$

Fig. 9a shows the laws of change of radius along the monopole, determined by the following formula (circle type, r_s is the radius of circle, see Fig. 1e)

$$r(s)=\begin{cases} r_0, \text{ at } s \le \kappa L - r_s \ \& \ s \ge \kappa L + r_s, \\ r_0 + [r_s^2 - (s-\kappa L)^2]/r_s, \text{at } s \ge \kappa L - r_s \ \& \ s \le \kappa L + r_s, \end{cases} \tag{12}$$

and Fig. 9b shows the dependences of the reflection coefficient modulus $|S_{11}|$ in the feeder line corresponding to these laws. As can be seen, the best matching is observed at $\kappa = 0.618$ and for the first time at $\kappa = 1.0$, an increase of the resonant frequency f_{res} is observed in comparison with a regular monopole ($\kappa = 0.0, r(s) = const$), in contrast to all previously considered laws of change in radius along the monopole.

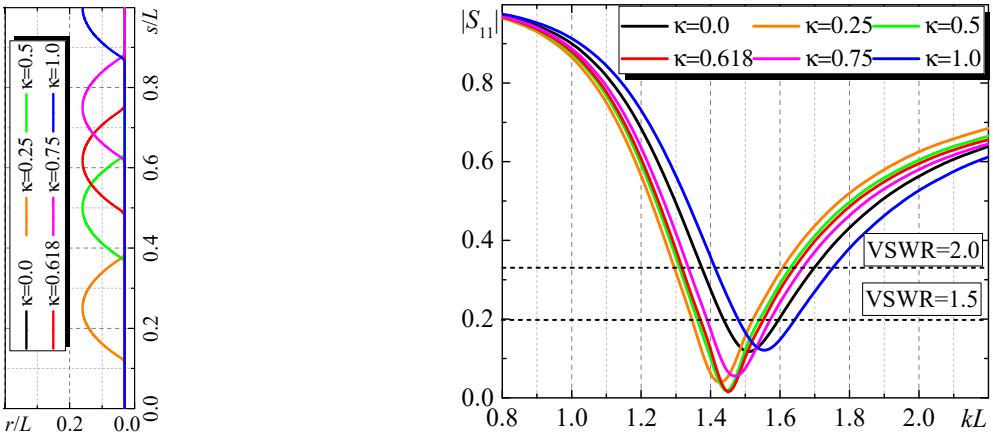

(a) (b)

Figure 9. The laws of change of radius along the monopole at $r_s = 6.516$ mm (a), the dependences of the reflection coefficient modulus $|S_{11}|$ in the feeder line from the electrical length of the monopole (b) for different κ

5. Numerical results for piecewise constant law of $r(s)$

Fig. 10a shows the laws of change of radius along the monopole, determined by the following formula (piecewise constant, $2h$ is the insert disc thickness, see Fig. 1f)

$$r(s)=\begin{cases} r_0, \text{ at } s \le \kappa L - h \ \& \ s \ge \kappa L + h, \\ r_m, \text{ at } s \in \kappa L \pm h, \end{cases} \tag{13}$$

and Fig. 10b shows the dependences of the reflection coefficient modulus $|S_{11}|$ in the feeder line corresponding to these laws. As can be seen, the best matching is observed at $\kappa = 0.75$ and at $\kappa = 1.0$ also increase in the resonant frequency f_{res} is observed in comparison with a regular monopole.

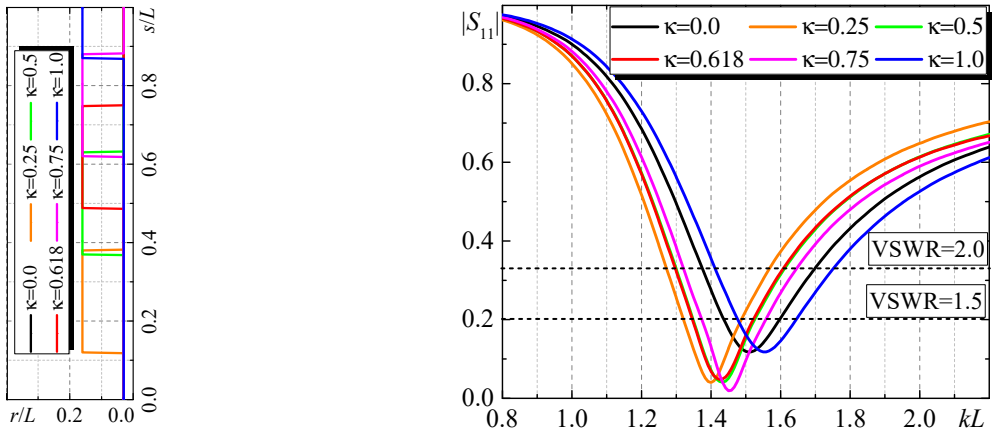

(a) (b)

Figure 10. The laws of change of radius along the monopole at $h = r_s = 6.516$ mm (a), the dependences of the reflection coefficient modulus $|S_{11}|$ in the feeder line from the electrical length of the monopole (b) for different κ

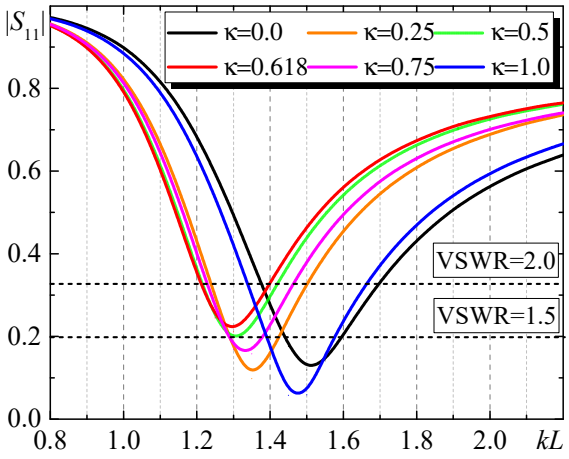

Figure 11. The dependences of the reflection coefficient modulus $|S_{11}|$ in the feeder line from the electrical length of the double-disk monopole structure for different κ at $h_n = 6.0$ mm ($n = 1 \div 6$)

If a second disk of the same or different thickness is added to one disk located at a certain distance along the length of the monopole, a double-disk structure is obtained. Obviously, instead of disks there can be any other structures (as well as their combinations) discussed above. Fig. 11 shows the dependences of the reflection coefficient modulus $|S_{11}|$ in the feeder line when the center of the first disk is located at point $\kappa_1 = s_m / L = 0.125$, and additional disks at $\kappa = 0.25; 0.5; 0.618; 0.75; 1.0$. The thicknesses of all disks are equal $2h$ =12.0 mm. As follows from the graphs, the best matching for this structure is observed (as before in Fig. 6) at $\kappa = 1.0$, and the greatest "shortening" of the monopole compared to that tuned monopole at $\kappa = 0.618$ (as before in Fig. 7).

TESTING OF THE ADEQUACY OF THE PROPOSED MATHEMATICAL MODEL TO A REAL PHYSICAL PROCESS

For testing of the adequacy of the proposed mathematical model to a real physical process, we briefly present numerical and experimental results for regular and conical dipoles located in a rectangular waveguide [24]. Let a dipole with a radius $r(s) = r_0 + |s| \tan\psi$ varying along the length (Fig. 12a) or a similar monopole (Fig.12b) be located in a rectangular waveguide with a cross-section $\{a \times b\}$.

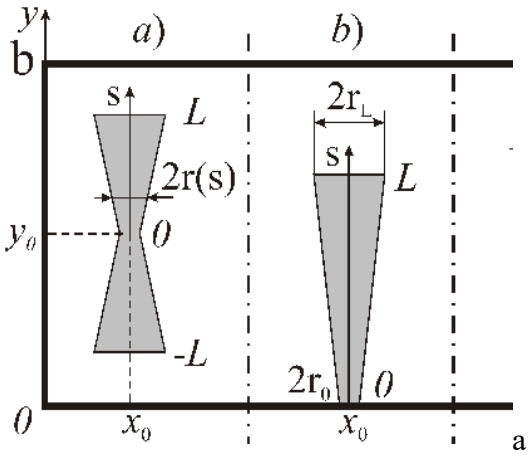

Figure 12. The geometries of the dipole (a) and monopole (b)

Then, when a fundamental type wave TE_{10} propagates in the waveguide, the reflection coefficient S_{11} from the monopole will be equal to

$$S_{11} = -\frac{4\pi i}{abk\gamma}\left(\frac{k}{\tilde{k}}\sin\frac{\pi x_0}{a}\right)^2 \frac{(\sin\tilde{k}L - \tilde{k}L\cos\tilde{k}L)^2}{Z_\psi^W(\tilde{k}L) + \mathrm{tg}\psi\tilde{Z}_\psi^W(\tilde{k}L) + \tilde{Z}_z(\tilde{k}L)}. \quad (14)$$

The solution is carried out by the generalized method of induced EMF with current approximation $J(s) = J_0(\cos\tilde{k}s - \cos\tilde{k}L)$). Expressions for the coefficients in formula (14) are presented in the Appendix I.

Fig. 13 shows the photographs of experimental samples of monopoles, which are located in the rectangular waveguide of size $\{a\times b\}$=58x25 mm^2. The axes of the monopoles are parallel to the narrow walls of the waveguide.

As can be seen, the value of the resonant wavelength λ_{res} for the conical dipole increases, correspondingly resonant frequency f_{res} is decreases, (curve 3) in comparison with the conductors of the constant radius (the curves 1, 2). Moreover, the radiuses of the latter equal to a smaller (curve 1) and a larger (curves 2) radiuses of the conical dipole, correspondingly. To our minds, this interesting fact is explained by the definite redistribution of energy of the near reactive fields between the E- and H-modes of the waveguide connected with the occurrence of some angle ψ between the axis $\{0y\}$ of the waveguide and $\{0s\}$ on the surface of the monopole. For the monopoles above the plane that we studied earlier, the same redistribution of reactive near fields obviously takes place.

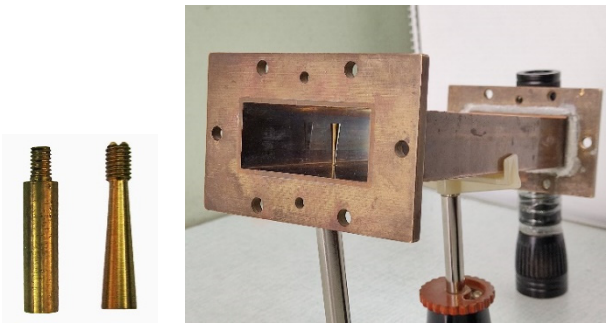

Figure 13. The experimental layouts of monopoles

Fig. 14 represents the dependences of the $|S_{11}|$ value on the wavelength for the cooper monopoles at L=15.0 mm, $x_0 = a/8$, $y_0 = 0$.

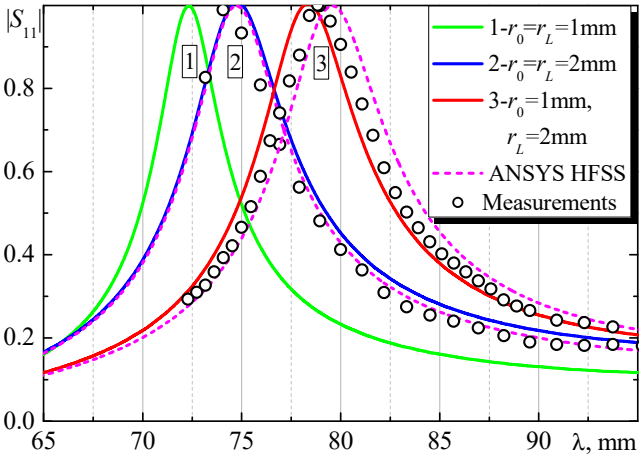

Figure 14. The dependences of the calculated and measured monopole reflection modulus $|S_{11}|$ in the waveguide at the constant and variable radiuses of their cross section: 1, 2, 3–calculation by the formula (12), 4–calculation by means of the package "ANSYS HFSS", 5–experimental data

CONCLUSION

Based on the obtained approximate analytical solution of the problem of current distribution along a radiating dipole with a variable cross-section radius, the input characteristics of a monopole over an infinite ideally conducting plane are investigated. It is shown that the use of different laws of radius variation along the monopole allows one to significantly improve the matching of the monopole with a feeder line with a standard characteristic impedance, and to change the resonant frequency of the monopole with its constant length. Thus, for successful matching of a monopole with a feeder line of a standard characteristic impedance, there is no need to change this impedance, but it is sufficient to change the antenna cross-section according to a certain law. This law can be chosen taking into account the requirements for changing or maintaining the resonant frequency of the radiator in comparison with the resonant frequency of a regular monopole.

It should be especially emphasized that, unlike the currently widely used commercial packages, in the presented solution it is sufficient to make the required changes to the analytical formulas, rather than drawing new structures each time. Moreover, the calculation time (using a computer based on Intel® Core™ i5-7200 processor) of input characteristics at one structure geometry using the proposed approach is about 0.5-1.0 seconds. The total time of calculation using a commercial ANSYS HFSS package, taking into account the finding of intermediate parameters, was approximately 2-3 minutes.

APPENDIX I

Coefficients in the formula (14):

$$Z_{\psi}^{W}(\tilde{k}L)=\frac{8\pi}{ab}\sum_{m=1}^{\infty}\sum_{n=0}^{\infty}\frac{\varepsilon_n(k^2-k_y^2)\tilde{k}}{kk_z(\tilde{k}^2-k_y^2)}e^{-k_z r_0}\sin^2 k_x x_0\cos^2 k_y y_0[\sin\tilde{k}L\cos k_y L-(\tilde{k}/k_y)\cos\tilde{k}L\sin k_y L]F_{\psi}(\tilde{k}L),$$

$$\tilde{Z}_{\psi}^{W}(\tilde{k}L)=\frac{4\pi}{ab}\sum_{m=1}^{\infty}\sum_{n=1}^{\infty}\frac{\tilde{k}^2}{k(\tilde{k}^2-k_y^2)}e^{-k_z r_0}\sin^2 k_x x_0[\cos\tilde{k}L(\cos k_y L-1)+(k_y/\tilde{k})\sin\tilde{k}L\sin k_y L+(k_y/\tilde{k})^2(\cos k_y L-1)]F_{\psi}(\tilde{k}L),$$

$$F_{\psi}(\tilde{k}L)=\frac{1/2}{(\tilde{k}+k_y)^2+(k_z\tan\psi)^2}\left\{e^{-k_z L\tan\psi}[(\tilde{k}+k_y)\sin(\tilde{k}+k_y)L-k_z\tan\psi\cos(\tilde{k}+k_y)L]+k_z\tan\psi\right\}$$

$$-\frac{\cos\tilde{k}L}{k_y^2+(k_z\tan\psi)^2}\left\{e^{-k_z L\tan\psi}[k_y\sin k_y L-k_z\tan\psi\cos k_y L]+k_z\tan\psi\right\}+\frac{1/2}{(\tilde{k}-k_y)^2+(k_z\tan\psi)^2}\left\{\begin{matrix}e^{-k_z L\tan\psi}[(\tilde{k}-k_y)\sin(\tilde{k}-k_y)L\\-k_z\tan\psi\cos(\tilde{k}-k_y)L]+k_z\tan\psi\end{matrix}\right\},$$

$\tilde{Z}_z(\tilde{k}L)=-\frac{i\omega z_l\sin 2\tilde{k}L}{2k\tilde{k}\cos\psi}$, $\varepsilon_n=\begin{cases}1, n=0\\2, n\neq 0\end{cases}$, $k_x=\frac{m\pi}{a}$, $k_y=\frac{n\pi}{b}$, $k_z=\sqrt{k_x^2+k_y^2-k^2}$, $\gamma=\sqrt{k^2-(\pi/a)^2}$, m and n are the integers.

ORCID

Mikhail V. Nesterenko, https://orcid.org/0000-0002-1297-9119; **Oleksandr M. Dumin,** https://orcid.org/0000-0001-5067-9689;
Yurii V. Arkusha, https://orcid.org/0000-0002-6483-4341

REFERENCES

[1] S. A. Schelkunoff, "Theory of antennas of arbitrary size and shape," Proc. IRE, **29**, 493-521 (1941). https://doi.org/10.1109/JRPROC.1941.231669
[2] C. T. Tai, "On the theory of biconical antennas," Journal Applied Phys., **19**, 1155-1160 (1948). https://doi.org/10.1063/1.1715036
[3] O. M. Woodward, and G. H. Brown, "Experimentally determined radiation characteristics of conical and triangular antenna," RCA (Radio Corp. Amer.) Rev., **13**, 425-453 (1952).
[4] R. M. Bevensee, *A Handbook of Conical Antennas and Scatterers*, (New York: Gordon and Breach, 1973).
[5] D. M. Bolle, and M. D. Morganstern, "Monopole and conic antennas on spherical vehicles," IEEE Trans. Antennas Propag., **17**, 477-484 (1969). https://doi.org/10.1109/TAP.1969.1139479
[6] T. T. Wu, and R. W. P. King, "The tapered antenna and its application to the junction problem for thin wires," IEEE Trans. Antennas Propag., **24**, 42-45 (1976). https://doi.org/10.1109/TAP.1976.1141274
[7] S. A. Saoudy, and M. Hamid, "Input admittance of a biconical antenna with wide feed gap," IEEE Trans. Antennas Propag., **38**, 1784-1790 (1990). https://doi.org/10.1109/8.102740
[8] S. S. Sandler, and R. W. P. King, "Compact conical antennas for wide-band coverage," IEEE Trans. Antennas Propag., **42**, 436-439 (1994). https://doi.org/10.1109/8.280735
[9] O. Givati, and A. P. C. Fourie, "Analysis of skeletal wire conical antennas" IEEE Trans. Antennas Propag., **44**, 844-858 (1996). https://doi.org/10.1109/8.509888
[10] F. E. S. Pereira, and M. H. C. Dias, "On the design of conical antennas for broadband impedance matching performance," Intern. J. Antennas Propag., 1-13 (2017).
[11] S. N. Samaddar, and E. L. Mokole, "Biconical antennas with unequal cone angles," IEEE Trans. Antennas Propag., **46**, 181-193 (1998). https://doi.org/10.1109/8.660962
[12] D. Ghosh, and T. K. Sarkar, "Design of a wide-angle biconical antenna for wideband communications," Prog. Electromagn. Res. B, **16**, 229-245 (2009). http://dx.doi.org/10.2528/PIERB09061508
[13] M. V. Nesterenko, V. A. Katrich, and S. V. Pshenichnaya, "Multiband asymmetric biconical dipole antenna with distributed surface impedance and arbitrary excitation," East European J. Physics, **2**, 450-455 (2024). https://doi.org/10.26565/2312-4334-2024-2-59
[14] M. V. Nesterenko, V. A. Katrich, Yu. V. Arkusha, and V. V. Katrich, "Radiation of electromagnetic waves by regular and biconical dipoles with variable distributed surface impedance and arbitrary excitation," East European J. Physics, **3**, 465-473 (2024). https://doi.org/10.26565/2312-4334-2024-3-56
[15] M. Nesterenko, V. Katrich, O. Dumin, and Yu. Arkusha, "Electrodynamic characteristics of biconical dipole with complex distributed surface impedance and asymmetric excitation," in Proc. XXIXth Int. Sem. Direct Inverse Problems of Electromagn. and Acoustic Wave Theory, 201-204 (2024). https://doi.org/10.1109/DIPED63529.2024.10706147
[16] M. V. Nesterenko, V. A. Katrich, S. V. Pshenichnaya, and S. A. Pogarsky, "Reducing influence of hardware of communication station on characteristics of asymmetric biconical dipole using magneto-dielectric substrate on finite-size metal screen," East European J. Physics, **2**, 424-430 (2025). https://doi.org/10.26565/2312-4334-2025-2-52
[17] K.-L. Wong, and S.-L. Chien, "Wide-band cylindrical monopole antenna for mobile phone," IEEE Trans. Antennas Propag., **53**, 2756-2758 (2005). https://doi.org/10.1109/TAP.2005.851784
[18] A. K. Amert, and K. W. Whites, "Miniaturization of the biconical antenna for ultrawideband applications," IEEE Trans. Antennas Propag., **57**, 3728-3735 (2009). https://doi.org/10.1109/TAP.2009.2026667
[19] C. S. Rao, and A. Sudhakar, "Analysis of edge terminated wide band biconical antenna," Access J., **30**, 804-809 (2015).
[20] F. F. Dubrovka, S. Piltyay, M. Movchan, and I. Zakharchuk, "Ultrawideband compact lightweight biconical antenna with capability of various polarizations reception for modern UAV applications," IEEE Trans. Antennas Propag., **71**, 2922-2929 (2023). https://doi.org/10.1109/TAP.2023.3247145
[21] D. B. Kuryliak, and O. M. Sharabura, "Diffraction of axially-symmetric TM-wave from bi-cone formed by finite and semi-infinite shoulders," Prog. Electromagn. Res. B, **68**, 73-88 (2016). http://dx.doi.org/10.2528/PIERB16041302
[22] O. Dumin, P. Fomin, V. Plakhtii, and M. Nesterenko, "Ultrawideband combined monopole-slot radiator of Clavin type," in Proc. XXVth Int. Sem. Direct Inverse Problems of Electromagn. and Acoustic Wave Theory, 32-36 (2020). https://doi.org/10.1109/DIPED49797.2020.9273399

[23] P. Fomin, O. Dumin, V. Plakhtii, and M. Nesterenko, "UWB antenna arrays with the monopole-slot radiator of Clavin type," in Proc. III-th Ukraine Conf. on Electrical and Computer Engineering, 258-261 (2021). https://doi.org/10.1109/UKRCON53503.2021.9575282
[24] M. V. Nesterenko, A. V. Gomozov, V. A. Katrich, S. L. Berdnik, and V. I. Kijko, "Scattering of electromagnetic waves by impedance biconical vibrators in a free space and in a rectangular waveguide," Prog. Electromagn. Res. C, **119**, 275-285 (2022). http://dx.doi.org/10.2528/PIERC22020304
[25] O. Dumin, V. Plakhtii, O. Skvortsova, and V. Katrich, "Tilted cone-enhanced ultrawideband monopole-slot radiators in antenna arrays," in Proc. XXIXth Int. Sem. Direct Inverse Problems of Electromagn. and Acoustic Wave Theory, 122-127 (2024). https://doi.org/10.1109/DIPED63529.2024.10706144
[26] M. V. Nesterenko, V. A. Katrich, Y. M. Penkin, V. M. Dakhov, and S. L. Berdnik, *Thin Impedance Vibrators. Theory and Applications*, (New York: Springer Science+Business Media, 2011). https://doi.org/10.1007/978-1-4419-7850-9
[27] T. W. Hertel, and G. Smith, "The insulated linear antenna-revisited," IEEE Trans. Antennas Propag., **48**, 914-920 (2000). https://doi.org/10.1109/8.865224
[28] S. A. Pogarsky, D. V. Mayboroda, and S. M. Mykhaliuk, "Influence of aperture of radiating strip structure on electrodynamic characteristics of patch antenna," East European J. Physics, 4, 274-280 (2023). https://doi.org/10.26565/2312-4334-2023-4-34
[29] M. Livio, *The Golden Ratio: The Story of PHI, the World's Most Astonishing Number*, (New York: Broadway Books, 2002).
[30] M. A. Barnes, "Ultra-wideband magnetic antenna," US patent 6,091,374, July 18, (2000).

ВХІДНІ ХАРАКТЕРИСТИКИ ЕЛЕКТРИЧНО ТОНКОГО ДИПОЛЯ ЗІ ЗМІННИМ РАДІУСОМ ВЗДОВЖ АНТЕНИ

М. В. Нестеренко, О. М. Думин, Ю. В. Аркуша
Харківський національний університет імені В.Н. Каразіна, майдан Свободи, 4, Харків, Україна, 61022

Представлено наближене аналітичне розв'язання задачі випромінювання (дифракції) електромагнітних хвиль диполем (монополем) зі змінним радіусом вздовж довжини антени. Розв'язання виконано з використанням узагальненого методу індукованих електрорушійних сил (ЕРС). Чисельно досліджено вплив зміни радіуса монополя на вхідні характеристики. Теоретичні результати порівнюються з експериментальними даними.

Ключові слова: *диполь; монополь; змінний радіус; вхідні характеристики; узагальнений метод наведених ЕРС*